

available at [www.sciencedirect.com](http://www.sciencedirect.com)

ScienceDirect

[www.elsevier.com/locate/molonc](http://www.elsevier.com/locate/molonc)

## Near infrared photoimmunotherapy of B-cell lymphoma



Tadanobu Nagaya, Yuko Nakamura, Kazuhide Sato, Toshiko Harada,  
Peter L. Choyke, Hisataka Kobayashi\*

Molecular Imaging Program, Center for Cancer Research, National Cancer Institute, National Institutes of Health,  
Bethesda, MD, 20892, United States

### ARTICLE INFO

#### Article history:

Received 25 May 2016

Received in revised form

19 July 2016

Accepted 22 July 2016

Available online 29 July 2016

#### Keywords:

Near infrared photoimmunotherapy  
CD20

B-cell lymphoma

Monoclonal antibodies

Near infrared light

Molecular imaging

### ABSTRACT

Near infrared photoimmunotherapy (NIR-PIT) is a new, highly-selective cancer theranostics that employs an antibody-photo absorber conjugate (APC). NIR-PIT has successfully treated preclinical tumor models with APCs and is now in the first-in-human phase 1 clinical trial for head and neck cancer patients against EGFR. CD20 is highly expressed in many B-cell lymphomas and is emerging as a molecular target for this disease. Here, we describe the use of the anti-CD20 monoclonal antibody (mAb), rituximab-IR700 APC for NIR-PIT of B-cell lymphoma in two CD20-expressing lymphoma mouse models. CD20 expressing B-cell lymphoma cell lines (Daudi and Ramos) were used in this study. Rituximab-IR700, rituximab conjugated with IRDye700DX, showed specific binding, and cell-specific killing only after exposure of NIR light to both cells *in vitro*. To evaluate effects of NIR-PIT *in vivo*, tumor-bearing mice were separated into 4 groups: (1) control; (2) APC *i.v.* only; (3) NIR light exposure only; (4) APC and NIR light (NIR-PIT). These were performed every week for up to 3 weeks. Rituximab-IR700 showed high tumor accumulation and high target-to-background ratio *in vivo*. Tumor growth was significantly inhibited by NIR-PIT in comparison with the other groups ( $p < 0.001$  for both tumors), and survival was significantly prolonged in both tumors ( $p < 0.001$  for Daudi tumors and  $p < 0.0001$  for Ramos tumors vs other groups). More than half of tumors were cured with this single regimen of NIR-PIT. In conclusion, anti-CD20 rituximab-IR700 works as a highly effective APC for NIR-PIT against B-cell lymphoma.

Published by Elsevier B.V. on behalf of Federation of European Biochemical Societies.

## 1. Introduction

CD20 is a B-cell antigen that is expressed from the late pre-B-cell stage until its loss just prior to terminal differentiation into plasma cells. CD20 is thought to have a regulatory function on

B-cell proliferation and differentiation (Tedder and Engel, 1994). As a cell surface protein, CD20 is highly expressed in many B-cell lymphomas, so CD20 has become an important target for antibody-based therapies of various B-cell lymphomas. Rituximab as an anti-CD20 monoclonal antibody

Abbreviations: ADCC, antibody-dependent cell-mediated cytotoxicity; APC, antibody-photo absorber conjugate; CD, cluster of differentiation; CDC, complement-dependent cytotoxicity; DIC, differential interference contrast; EGFR, epidermal growth factor receptor; FDA, Food and Drug Administration; H&E, hematoxylin and eosin; IR700, IRDye700DX; LED, light-emitting diode; mAb, monoclonal antibody; NIR, near infrared; PI, propidium iodide; PBS, phosphate buffered saline; PIT, photoimmunotherapy; ROI, regions of interest; SDS-PAGE, sodium dodecyl sulfate-polyacrylamide gel electrophoresis; TBR, target-to-background ratio.

\* Corresponding author. Fax: +1 3014023191.

E-mail address: [kobayash@mail.nih.gov](mailto:kobayash@mail.nih.gov) (H. Kobayashi).

<http://dx.doi.org/10.1016/j.molonc.2016.07.010>

1574-7891/Published by Elsevier B.V. on behalf of Federation of European Biochemical Societies.

(mAb) is the first commercial antibody for treating malignancy which was approved by the Food and Drug Administration (FDA) (Leget and Czuczman, 1998). The anti-tumor activity of rituximab relies on antibody-dependent cell-mediated cytotoxicity (ADCC) and complement-dependent cytotoxicity (CDC) (Hamaguchi et al., 2006; Lefebvre et al., 2006; Reff et al., 1994; Uchida et al., 2004). Thus, rituximab, in combination with chemotherapy, has become an effective first-line or salvage therapy for B-cell lymphomas (Economopoulos et al., 2003; Griffin et al., 2009; Marcus et al., 2005; Wildes et al., 2014). However, such treatments are not curative in all patients, especially those with aggressive malignancies (Wasterlid et al., 2011, 2013).

Burkitt's lymphoma is a rare, highly aggressive type of mature B-cell neoplasm, accounting for approximately 1–2% of adult and 30–40% of childhood non-Hodgkin's lymphoma. Although much progress has been made, Burkitt's lymphoma remains a difficult disease to treat among B-cell lymphomas (Molyneux et al., 2012). For instance, conventional therapeutic regimens used in non-Hodgkin's lymphoma such as CHOP (cyclophosphamide, doxorubicin, vincristine, and prednisone) have not been universally successful in patients with Burkitt's lymphoma (Wildes et al., 2014). Short, intensive regimens result in CR rates of 70–90%, and long-term event-free survival (EFS) rates between 45% and 90% (Wildes et al., 2014). However, this intensive multi-drug chemotherapy regimen also causes severe toxic side-effects including long lasting hematologic toxicity and mucositis that increase the risk of severe infection or chemotherapy-associated secondary neoplasm. Relapses after this and other intensive therapies are often lethal.

Near infrared photoimmunotherapy (NIR-PIT) is a tumor theranostics that employs a targeted monoclonal antibody-photo absorber conjugate (APC) including IRDye700DX (IR700, silica-phthalocyanine dye). NIR-PIT has been shown to be highly effective and selective (Mitsunaga et al., 2011). Unlike intensive chemotherapy, non-target expressing cells suffer no toxic effects after NIR-PIT. A first-in-human Phase 1 trial of NIR-PIT with an APC targeting epidermal growth factor receptor (EGFR) in patients with inoperable head and neck cancer was approved by the US FDA, and is underway (<https://clinicaltrials.gov/ct2/show/NCT02422979>).

NIR-PIT has been shown to be effective with a variety of different APCs however, anti-CD20, a commonly used antibody, has not been tested as an APC for NIR-PIT (Hanaoka et al., 2015; Mitsunaga et al., 2011; Nagaya et al., 2015, 2016b; Sato et al., 2015; Watanabe et al., 2015). In this study, we performed *in vitro* tumor binding, *in vivo* tumor accumulation and intratumoral distribution studies in animal models using two human aggressive B-cell (Burkitt's) lymphoma cell lines (Daudi and Ramos). Following this, NIR-PIT was performed with rituximab-IR700 *in vitro* and in two tumor bearing mouse models *in vivo* and efficacy was established.

## 2. Materials and methods

### 2.1. Reagents

Water soluble, silica-phthalocyanine derivative, IRDye700DX NHS ester was obtained from LI-COR Biosciences (Lincoln,

NE, USA). Rituximab, a chimeric (mouse/human) monoclonal antibody (mAb) directed against CD20 was purchased from Genentech (South San Francisco, CA, USA). All other chemicals were of reagent grade.

### 2.2. Synthesis of IR700-conjugated rituximab

Conjugation of dyes with mAb was performed according to previous methods (Mitsunaga et al., 2011). In brief, rituximab (1.0 mg, 7 nmol) was incubated with IR700 NHS ester (61.1  $\mu$ g, 31.3 nmol) in 0.1 M Na<sub>2</sub>HPO<sub>4</sub> (pH 8.6) at room temperature for 1 h. The mixture was purified with a Sephadex G25 column (PD-10; GE Healthcare, Piscataway, NJ, USA). The protein concentration was determined with Coomassie Plus protein assay kit (Thermo Fisher Scientific Inc, Rockford, IL, USA) by measuring the absorption at 595 nm with UV-Vis (8453 Value System; Agilent Technologies, Santa Clara, CA, USA). The concentration of IR700 was measured by absorption at 689 nm to confirm the number of fluorophore molecules per mAb. The synthesis was controlled so that an average of two IR700 molecules was bound to a single antibody. We abbreviate IR700 conjugated to rituximab as rit-IR700. As a quality control for the conjugate, we performed sodium dodecyl sulfate-polyacrylamide gel electrophoresis (SDS-PAGE). The conjugate was separated by SDS-PAGE with a 4–20% gradient polyacrylamide gel (Life technologies, Gaithersburg, MD). A standard marker (Crystalgen Inc., Com-mack, NY) was used as a protein marker of molecular weight. After electrophoresis at 80 V for 2.5 h, the gel was imaged with a Pearl Imager (LI-COR Biosciences, Lincoln, Nebraska, USA) using a 700 nm fluorescence channel. We used diluted rituximab as a control. The gel was stained with Colloidal Blue staining to determine the molecular weight of the conjugate.

### 2.3. Cell culture

Epstein–Barr virus negative B-cell lymphoma cell lines, Daudi and Ramos, were purchased from American type culture collection (ATCC; Manassas, VA, USA). Cells were grown in RPMI 1640 (Life Technologies, Gaithersburg, MD, USA) supplemented with 10% fetal bovine serum and 1% penicillin/streptomycin (Life Technologies) in tissue culture flasks in a humidified incubator at 37 °C at an atmosphere of 95% air and 5% carbon dioxide.

### 2.4. Flow cytometry

To verify *in vitro* rit-IR700 binding, fluorescence from cells after incubation with the APC was measured using a flow cytometer (FACS Calibur, BD BioSciences, San Jose, CA, USA) and CellQuest software (BD BioSciences). Daudi and Ramos cells ( $4 \times 10^5$ ) were seeded into 12 well plates and incubated for 24 h. Rit-IR700 was then added to the culture medium at 10  $\mu$ g/ml and incubated for 6 h at 37 °C. To validate the specific binding of the conjugated antibody, excess antibody (100  $\mu$ g) was used to block 10  $\mu$ g of APCs.

## 2.5. Fluorescence microscopy

To detect the antigen specific localization and effect of NIR-PIT, fluorescence microscopy was performed (BX61; Olympus America, Inc., Melville, NY, USA). Twenty thousand cells were seeded into 6 well plates and incubated for 24 h. Rit-IR700 was then added to the culture medium at 10  $\mu\text{g/ml}$  and incubated for 6 h at 37 °C. After incubation the cells were washed with phosphate buffered saline (PBS). The filter set to detect IR700 consisted of a 590–650 nm excitation filter, a 665–740 nm band pass emission filter. Transmitted light differential interference contrast (DIC) images were also acquired.

## 2.6. In vitro NIR-PIT

The cytotoxic effects of NIR-PIT with rit-IR700 were determined by flow cytometric Propidium Iodide (PI) (Life Technologies) staining, which detects compromised cell membranes. Four hundred thousand cells were seeded into 12 well plates and incubated for 24 h. Rit-IR700 was then added to the culture medium at 10  $\mu\text{g/ml}$  and incubated for 6 h at 37 °C. After washing with PBS, PBS was added. Then, cells were irradiated with a red light-emitting diode (LED), which emits light at 670–710 nm wavelength (L690-66-60; Marubeni America Co., Santa Clara, CA, USA), at a power density of 50  $\text{mW/cm}^2$  as measured with an optical power meter (PM 100, Thorlabs, Newton, NJ, USA). Cells were harvested 1 h after treatment. Then PI was added in the cell suspension (final 2  $\mu\text{g/ml}$ ) and incubated at room temperature for 30 min, followed by flow cytometry. Each value represents mean  $\pm$  standard error of the mean (s.e.m.) of five experiments.

## 2.7. Animal and tumor models

All *in vivo* procedures were conducted in compliance with the Guide for the Care and Use of Laboratory Animal Resources (1996), US National Research Council, and approved by the local Animal Care and Use Committee. Six to eight week old female homozygote athymic nude mice were purchased from Charles River (NCI-Frederick, Frederick, MD). During the procedure, mice were anesthetized with isoflurane. In order to determine tumor volume, the greatest longitudinal diameter (length) and the greatest transverse diameter (width) were measured with an external caliper. Tumor volumes were based on caliper measurements and were calculated using the following formula; tumor volume = length  $\times$  width<sup>2</sup>  $\times$  0.5. Body weight was also measured. Mice were monitored daily for their general health and tumor volumes were measured three times a week until the tumor volume reached 2000  $\text{mm}^3$ , whereupon the mice were euthanized with inhalation of carbon dioxide gas.

## 2.8. In vivo fluorescence imaging studies

Daudi and Ramos cells ( $1 \times 10^7$ ) were injected subcutaneously in the right dorsum of the mice. Tumors were studied after they reached volumes of approximately 50  $\text{mm}^3$ . Serial dorsal fluorescence images of IR700 were obtained with a Pearl Imager using a 700 nm fluorescence channel before and 0, 1/2, 1, 2, 3, 4, 5, 6, 9, 12, 24, 48, 72, 96, 120, 144, and 168 h after i.v.

injection of 100  $\mu\text{g}$  of rit-IR700 via the tail vein. Pearl Cam Software (LICOR Biosciences) was used for analyzing fluorescence intensities. Region of interests (ROIs) were placed on the tumor. ROIs were also placed in the adjacent non-tumor region as background (left dorsum). Average fluorescence intensity of each ROI was calculated. Target-to-background ratio (TBR) (fluorescence intensities of target/fluorescence intensities of background) were also calculated ( $n = 10$ ).

## 2.9. In vivo NIR-PIT

Daudi and Ramos cells ( $1 \times 10^7$ ) were injected subcutaneously in the right dorsum of the mice. Tumors were studied after they reached volumes of approximately 50  $\text{mm}^3$ . To examine the therapeutic effect of *in vivo* NIR-PIT on both cells, tumor bearing mice were randomized into 4 groups of at least 8 animals per group for the following treatments: (1) no treatment (control); (2) 100  $\mu\text{g}$  of rit-IR700 i.v., no NIR light exposure (APC i.v. only); (3) NIR light exposure only, NIR light was administered at 50  $\text{J/cm}^2$  on day 1 and 100  $\text{J/cm}^2$  on day 2 (NIR light only); (4) 100  $\mu\text{g}$  of rit-IR700 i.v., NIR light was administered at 50  $\text{J/cm}^2$  on day 1 after injection and 100  $\text{J/cm}^2$  on day 2 after injection (NIR-PIT). These therapies were performed every week for up to 3 weeks. Serial fluorescence images, as well as white light images, were obtained before and after each NIR light exposure (day 0, day 1 and day 2) using a Pearl Imager with a 700 nm fluorescence channel.

## 2.10. Histological analysis

To detect the antigen specific micro-distribution in the tumor, fluorescence microscopy was performed. Tumor xenografts were excised from mice without treatment, 24 h after injection of rit-IR700 (APC i.v. only) and 24 h after NIR-PIT. Extracted tumors were frozen with OCT compound (SAKURA Finetek Japan Co., Tokyo, Japan) and frozen sections (10  $\mu\text{m}$  thick) were prepared. Fluorescence microscopy was performed using the BX61 microscope with the following filters; excitation wavelength 590–650 nm, emission wavelength 665–740 nm long pass for IR700 fluorescence. DIC images were also acquired. To evaluate histological changes light microscopy study was also performed using Olympus BX61. Extracted tumors were also placed in 10% formalin and serial 10  $\mu\text{m}$  slice sections were fixed on glass slide with hematoxylin and eosin (H&E) staining.

## 2.11. Statistical analysis

Data are expressed as means  $\pm$  s.e.m. from a minimum of five experiments, unless otherwise indicated. Statistical analyses were carried out using GraphPad Prism version 6 (GraphPad Software, La Jolla, CA, USA). For multiple comparisons, a one-way analysis of variance (ANOVA) followed by the Bonferroni correction for multiple comparisons was used. The cumulative probability of survival based on volume (2000  $\text{mm}^3$ ) was estimated in each group with a Kaplan–Meier survival curve analysis, and the results were compared with use of the log-rank test. Student's *t* test was used to compare the treatment effects with that of control *in vitro*. To compare intensity and TBR between Daudi and Ramos tumors at all

time points, the Mann–Whitney-U test was used.  $p$ -value of  $<0.05$  was considered statistically significant.

### 3. Results

#### 3.1. In vitro characterization of lymphoma cells

As defined by SDS-PAGE, rit-IR700 and non-conjugated control mAb showed an identical molecular weight, around 150 kDa, and fluorescence intensity was confirmed in the band of rit-IR700 (Figure 1A). After a 6 h incubation with rit-IR700, Daudi and Ramos cells showed high fluorescence signal, which was confirmed with flow cytometry (Figure 1B and C) and fluorescence microscopy (Figure 1D). These signals were completely blocked by adding excess rituximab, indicating that the APC specifically binds to CD20 on both cells (Figure 1B and C).

#### 3.2. In vitro NIR-PIT

Immediately after exposure, NIR light induced cellular swelling, bleb formation, and rupture of vesicles representing

necrotic cell death (Suppl. Videos S1 and S2). Most of these morphologic changes were observed within 15 min of light exposure in both cells (Figure 1D). Based on incorporation of PI staining, percentage of cell death increased in a light dose dependent manner (Figure 1E and F). There was no significant cytotoxicity associated with NIR light alone in the absence of APC and with APC alone without NIR light in both cells. Percentage of cell death in Daudi cells was higher than that in Ramos cells at the same light dose. For instance, when exposed to 8 J of NIR light the percentage of cell death in Daudi cells was over 80% (Figure 1E), while it was only 40% in Ramos cells (Figure 1F).

Supplementary video related to this article can be found at <http://dx.doi.org/10.1016/j.molonc.2016.07.010>.

#### 3.3. In vivo fluorescence imaging studies

Moderate fluorescence intensity from rit-IR700 was observed in Daudi tumors within 12 h after APC injection after which the fluorescence intensity gradually decreased. Superior fluorescence intensity from rit-IR700 was observed in Ramos

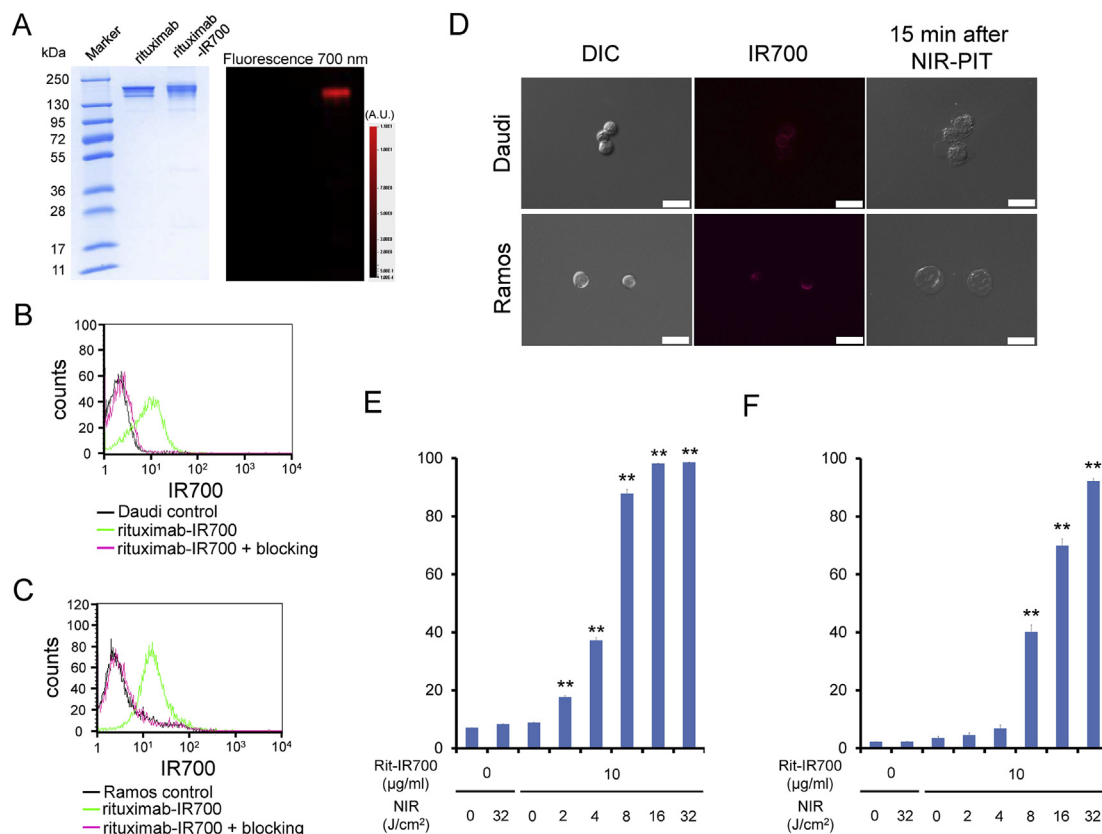


**Figure 1** – Confirmation of CD20 expression as a target for NIR-PIT in Ramos and Daudi cells, and evaluation of *in vitro* NIR-PIT. (A) Validation of rit-IR700 by SDS-PAGE (left: Colloidal Blue staining, right: fluorescence). Diluted rituximab was used as a control. (B) Expression of CD20 in Daudi cells was evaluated by FACS. After 6 h of rit-IR700 incubation, Daudi cells showed high fluorescence signal. (C) Expression of CD20 in Ramos cells was examined with FACS. After 6 h of rit-IR700 incubation, Ramos cells showed high fluorescence signal. (D) Differential interference contrast (DIC) and fluorescence microscopy images of Daudi and Ramos cells after incubation with rit-IR700 for 6 h. High fluorescence intensities were shown in both cells. Necrotic cell death was observed upon excitation with NIR light (after 15 min) in both cells. Scale bars = 20 μm. (E) Membrane damage of Daudi cells induced by NIR-PIT was measured with the dead cell count using PI staining, which increased in a light dose dependent manner ( $n = 5$ ,  $**p < 0.001$ , vs untreated control, by Student's  $t$  test). (F) PI staining showed membrane damage of Ramos cells ( $n = 5$ ,  $**p < 0.001$ , vs untreated control, by Student's  $t$  test).

tumors, however, it was delayed compared to Daudi cells, reaching its peak within 1 day after APC injection and thereafter gradually decreasing over the following days (Figure 2A and B). The fluorescence intensities were significantly higher in Ramos tumors compared with Daudi tumors between 1 day and 7 days after APC injection ( $p < 0.01$  at all time points). TBR of rit-IR700 in Ramos tumors increased within three days after APC injection then the TBR decreased slightly. On the other hand, TBR of rit-IR700 in Daudi tumors decreased beginning 12 h after APC injection (Figure 2C). TBRs were also significantly higher in Ramos tumors compared to Daudi tumors between 1 day and 7 days after APC injection ( $p < 0.01$  at all time points).

### 3.4. In vivo NIR-PIT for Daudi tumor model

The treatment and imaging regimen for Daudi tumors is shown in Figure 3A. One day after injection of rit-IR700, the

tumor showed higher fluorescence intensity than did the tumor with no APC. Immediately after exposure to 50 J/cm<sup>2</sup> of NIR light, IR700 fluorescence signal of tumor decreased due to dying cells and partial photo-bleaching. In mice receiving rit-IR700 but no NIR light the IR700 fluorescence continued to decrease over the following days due to clearance (Figure 3B). Tumor growth was inhibited and survival was prolonged significantly in the NIR-PIT group compared with the other groups ( $p < 0.001$ ) (Figure 3C and D). No significant therapeutic effect was observed in the control groups including those receiving APC i.v. only or in mice receiving the NIR light only. There was no skin necrosis or toxicity attributable to the APC in any group.

### 3.5. Histological analysis for Daudi tumor

The treatment regimen is shown in Figure 4A. In frozen histologic specimens, high fluorescence intensity was shown in

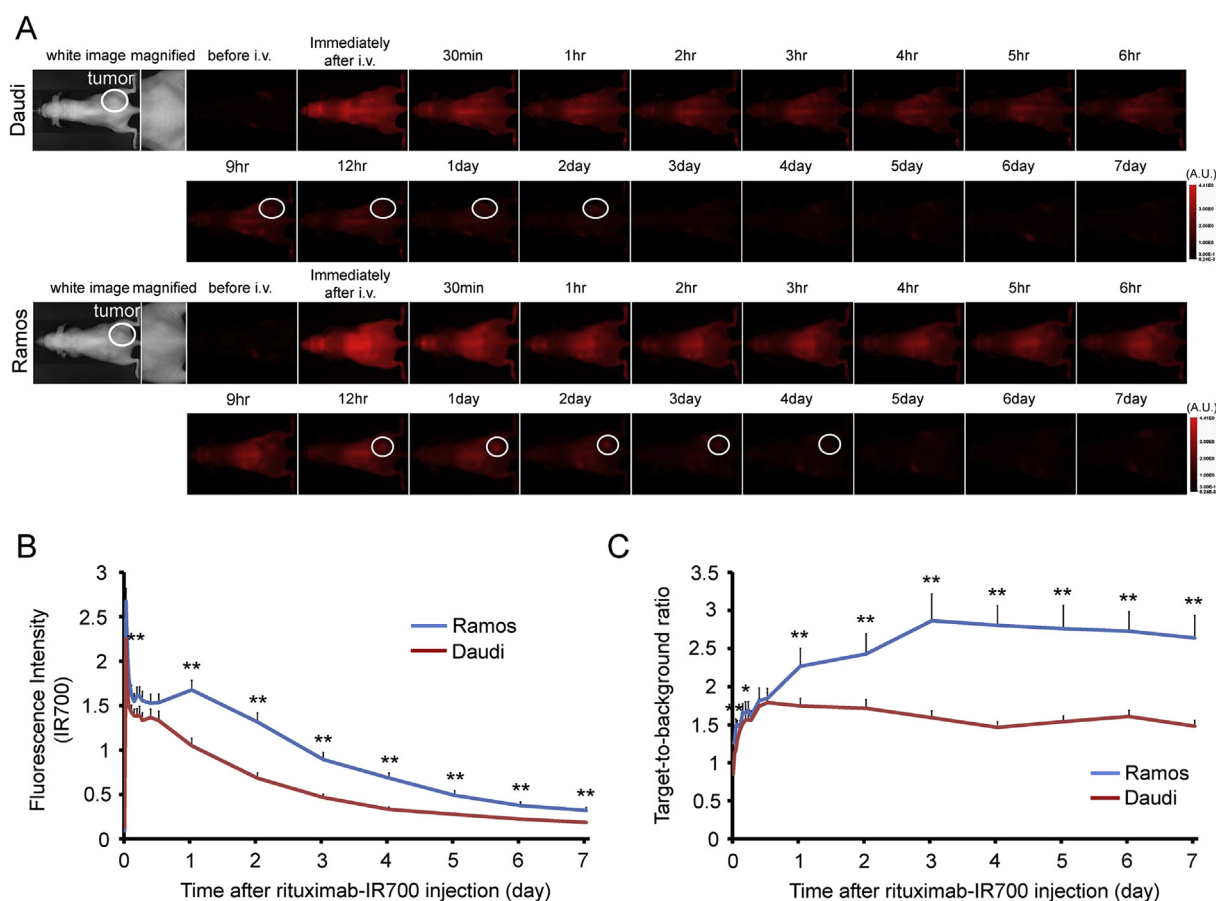
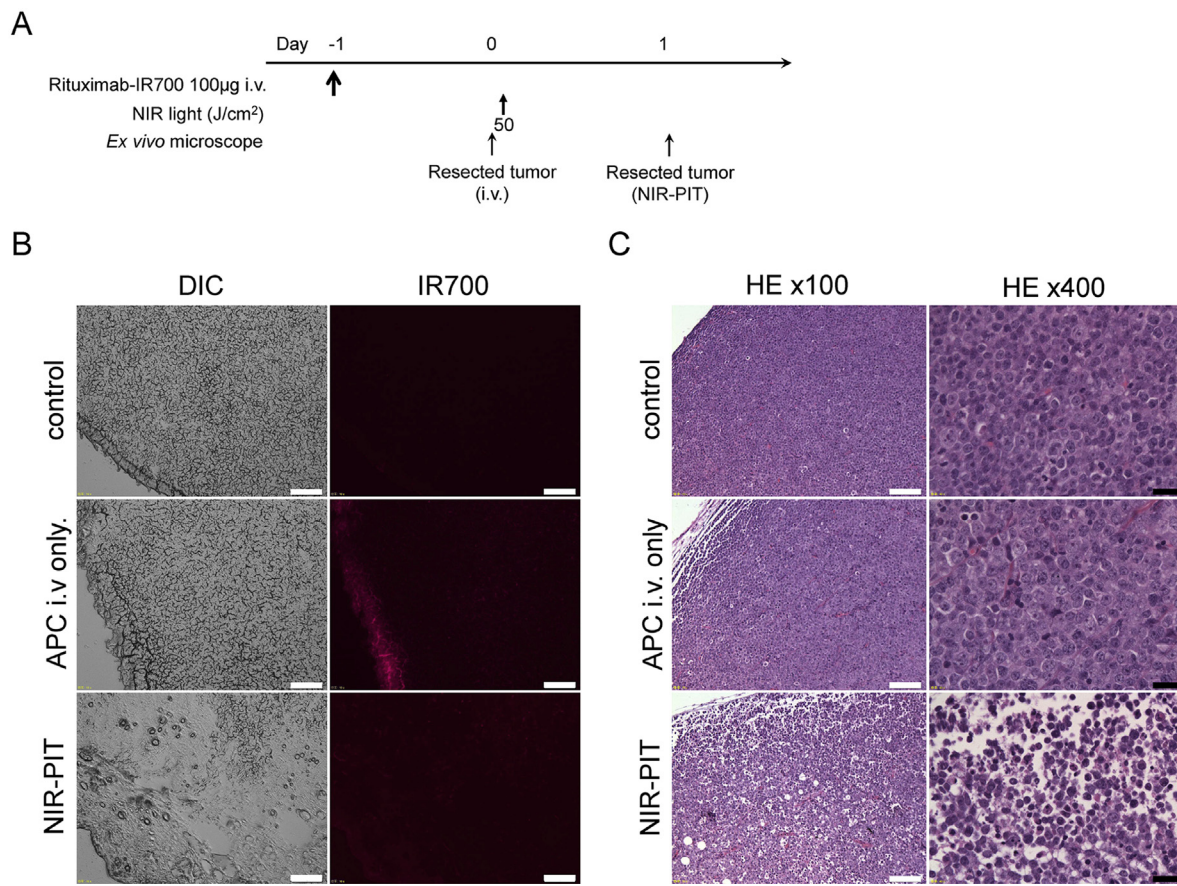


Figure 2 – *In vivo* fluorescence imaging of Ramos and Daudi tumor. (A) *In vivo* rit-IR700 fluorescence real-time imaging of tumor bearing mice (right dorsum). The fluorescence intensity of rit-IR700 in both Ramos and Daudi tumor gradually decreased over days. The fluorescence intensity of IR700 was higher in Ramos tumor compared with Daudi tumor. (B) Quantitative analysis of IR700 intensities in both tumors ( $n = 10$ ). The IR700 fluorescence intensity of rit-IR700 in Daudi tumors showed high intensities within 12 h after APC injection then the fluorescence intensity gradually decreased, while the fluorescence intensity of rit-IR700 in Ramos tumors showed higher intensities within 1 day after APC injection before decreasing gradually over the following days. The overall IR700 fluorescence intensity over time was significantly higher in Ramos tumors compared with Daudi tumors at most time points (\*\* $p < 0.01$ , by Mann–Whitney–U test). (C) Quantitative analysis of TBR in both tumors ( $n = 10$ ). TBR of rit-IR700 in Ramos tumors increased within three days after APC injection then decreased slightly. On the other hand, TBR of rit-IR700 in Daudi tumors started to decrease as early as 12 h after APC injection. TBRs of Ramos tumors were significantly higher than Daudi tumors at most time points (\* $p < 0.05$ , \*\* $p < 0.01$ , by Mann–Whitney–U test).





**Figure 4** – *In vivo* histological fluorescence distribution and histological NIR-PIT effect of Daudi tumor. (A) The regimen of NIR-PIT is shown. (B) Differential interference contrast (DIC) and fluorescence microscopy images of Daudi tumors. High fluorescence intensity is shown in Daudi tumor 24 h after injection of rit-IR700, but the fluorescence decreased 24 h after NIR-PIT. Scale bars = 100 µm. (C) Resected tumor stained with hematoxylin and eosin (H&E). A few scattered clusters of damaged tumor cells are seen within a background of diffuse cellular necrosis and micro-hemorrhage after NIR-PIT, while no obvious damage was observed after rit-IR700 alone with NIR light. White scale bars = 100 µm. Black scale bars = 20 µm.

IR700 but no NIR light, the IR700 fluorescence gradually decreased over the following days (Figure 5B). Tumor growth was significantly inhibited in the NIR-PIT treatment group compared with the other groups ( $p < 0.001$ ) (Figure 5C). Additionally, significantly prolonged survival was achieved in the NIR-PIT group ( $p < 0.0001$  vs other groups) (Figure 5D). No significant therapeutic effect was observed in the control groups including those receiving APC only or in mice receiving NIR light only. There was no skin necrosis or toxicity attributable to the APC in any group.

### 3.7. Histological analysis for Ramos tumor

The treatment regimen is shown in Figure 6A. In frozen histologic specimens, high fluorescence intensity was shown in Daudi tumors 24 h after rit-IR700 injection compared with that in control tumors. On the other hand, the majority of fluorescence signal in Ramos tumors disappeared within 24 h after NIR-PIT (Figure 6B). H&E staining of NIR-PIT treated tumors revealed diffuse necrosis and micro-hemorrhage, with scattered clusters of live but damaged tumor cells, while no

obvious damage was observed in the tumor receiving only rit-IR700 but no light (Figure 6C).

## 4. Discussion

CD20, a B-cell antigen, is highly expressed in the majority of B-cell lymphoma cells. Additionally, CD20 is not shed or internalized, suggesting that CD20 is an excellent therapeutic target for NIR-PIT which specifically damages cell membranes. Efficient binding and distribution of the antibody in the tumor are important for APCs to be effective as agents for NIR-PIT as heterogeneity will lead to undertreatment of regions of the tumor. Our results showed that the rituximab-based APC, rit-IR700, bound to CD20 specifically and there was little internalization within 6 h of incubation in cells. The APC also showed high tumor TBRs in *in vivo* tumor models as shown in Figure 2, indicating that APC accumulated to a sufficient degree for treating tumors. These results suggest that rituximab has favorable characteristics as an APC for NIR-PIT. When CD20 expressing lymphomas were treated

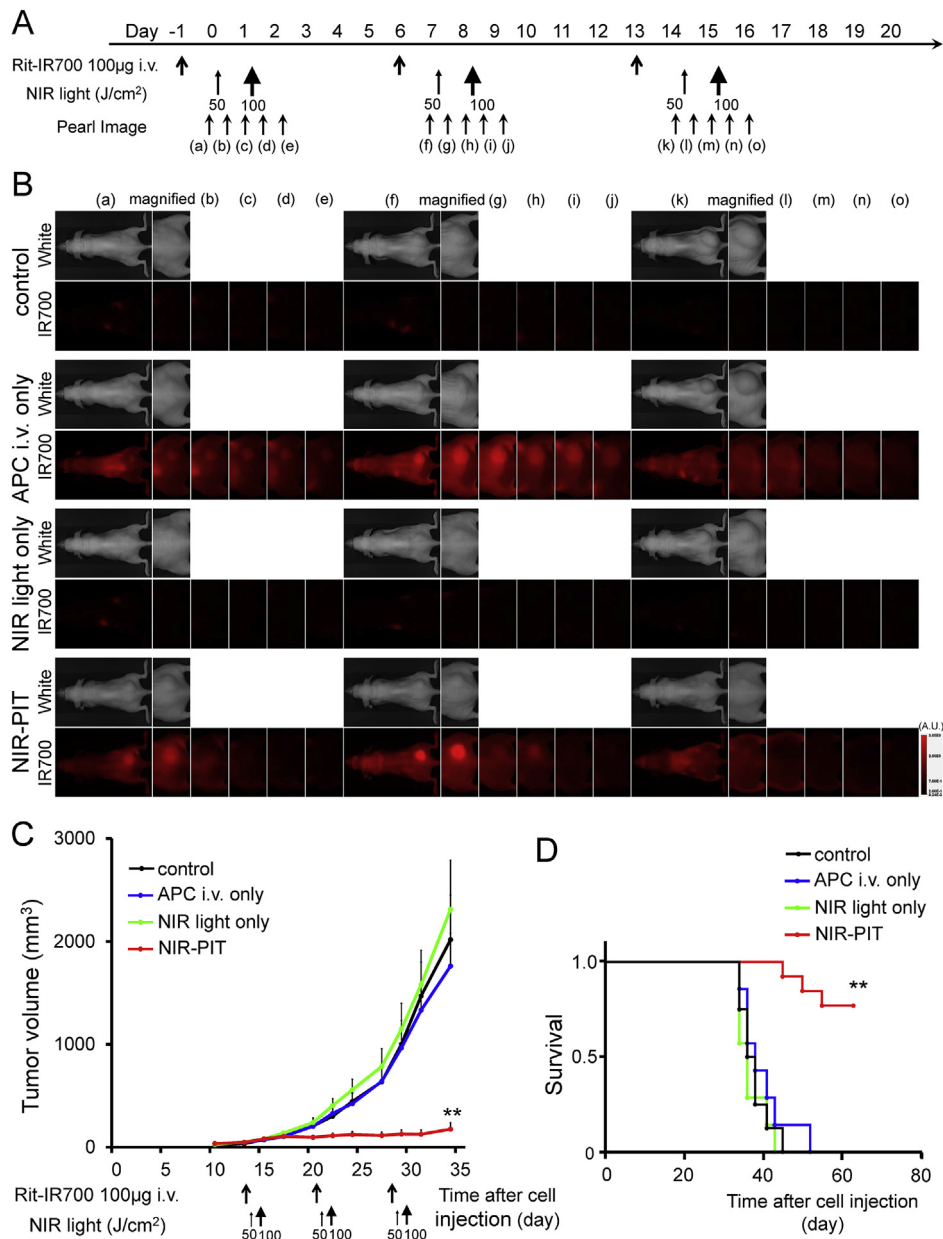


**Figure 5** – *In vivo* effect of NIR-PIT for Ramos tumor. (A) NIR-PIT regimen. Fluorescence images were obtained at each time point as indicated. (B) *In vivo* fluorescence real-time imaging of Ramos tumor bearing mice in response to NIR-PIT. The tumor treated by NIR-PIT showed decreasing IR700 fluorescence after NIR-PIT. (C) Tumor growth was significantly inhibited in the NIR-PIT treatment group with rit-IR700 ( $n = 8-10$ ,  $**p < 0.001$  vs other groups, Bonferroni's test with ANOVA). (D) Significantly prolonged survival was observed in NIR-PIT treatment group with rit-IR700 ( $n = 8-10$ ,  $*p < 0.0001$  vs other groups, by Log-rank test).

with rit-IR700 NIR-PIT, rapid cell death was found *in vitro* and tumor growth inhibition and survival improvements were demonstrated *in vivo*. Thus, rit-IR700 NIR-PIT is a potentially effective approach to treating CD20 expressing lymphomas.

From the pharmacokinetic point of view, malignant lymphoma generally shows favorable homogeneous distribution of antibodies in tumors. IR700 conjugation minimally alters the pharmacokinetics of the antibody due its small size compared to the antibody and the hydrophilic nature of the IR700 dye. As a result, these APCs show highly targeted accumulation in the tumor and specific binding to target cells with minimal distribution in normal tissue and minimal binding to

non-target expressing cells. Therefore, NIR-PIT can be used to selectively kill a variety of different tumor types depending on the targeting properties of the antibody employed (Hanaoka et al., 2015; Mitsunaga et al., 2011; Nagaya et al., 2015, 2016b; Sato et al., 2015; Watanabe et al., 2015).

Rapid cell killing of perivascular tumor with NIR-PIT leads to an immediate increase in vascular permeability. This is known as the super enhanced permeability and retention (SUPR) effect (Kobayashi et al., 2013; Sano et al., 2013, 2014). The delivery of various nano-sized or macromolecular drugs is increased up to 24-fold compared to baseline after the initial NIR exposure. After the first NIR-PIT, circulating APC can

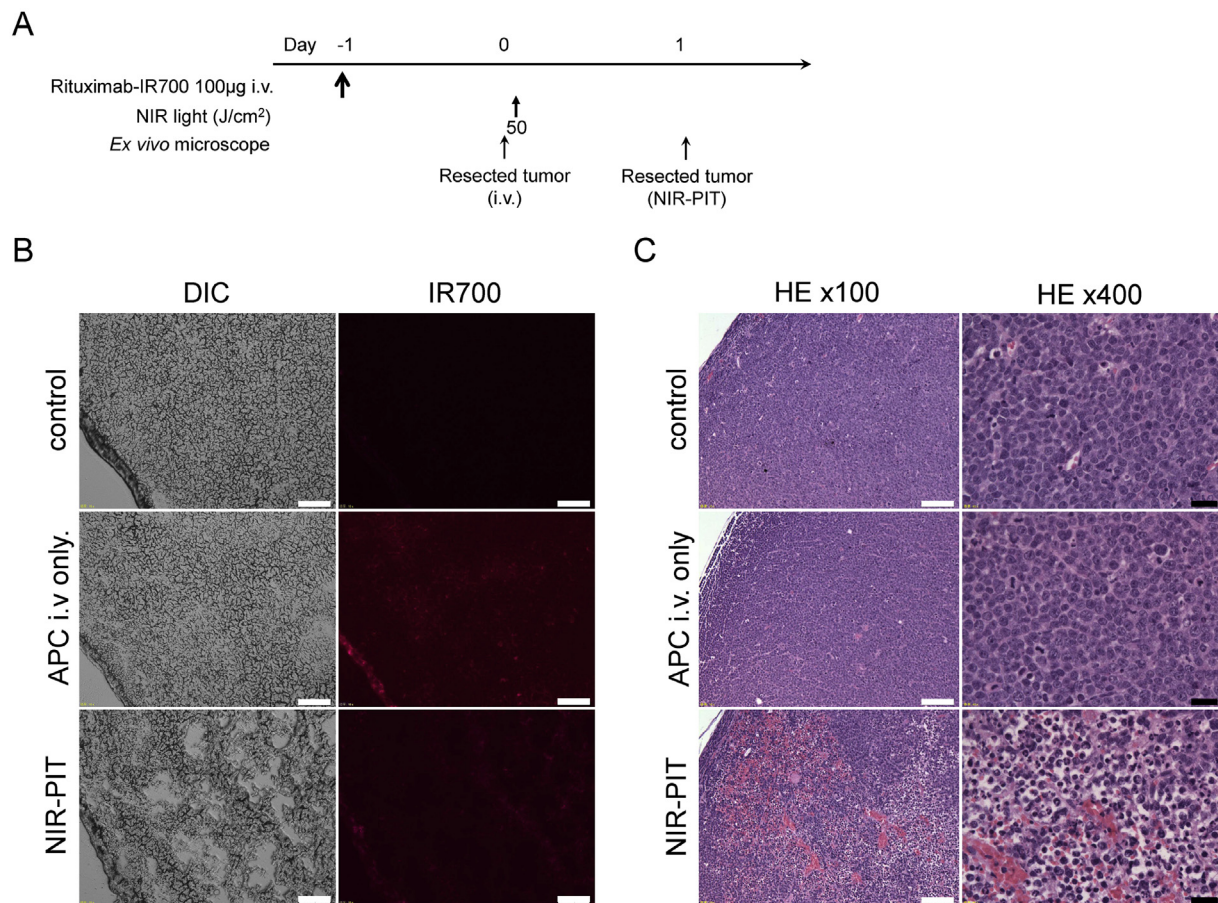


**Figure 6** – *In vivo* histological fluorescence distribution and histological NIR-PIT effect of Ramos tumor. (A) The regimen of NIR-PIT. (B) Differential interference contrast (DIC) and fluorescence microscopy images of Ramos tumors. High fluorescence intensity is shown in Ramos tumor 24 h after injection of rit-IR700, but the fluorescence decreased 24 h after NIR-PIT. Scale bars = 100 µm. (C) Resected tumor stained with hematoxylin and eosin (H&E). A few scattered clusters of damaged tumor cells are seen within a background of diffuse cellular necrosis and micro-hemorrhage after NIR-PIT, while no obvious damage was observed after rit-IR700 alone with NIR light. White scale bars = 100 µm. Black scale bars = 20 µm.

permeate more deeply into the treated tumor's extravascular space due to the SUPR effect, enabling targeting of tumor cells that were sequestered from APC binding prior to NIR-PIT. Therefore, the second exposure to NIR light can further enhance therapeutic effects of NIR-PIT (Mitsunaga et al., 2012; Nagaya et al., 2016a). Thus, we chose the current therapeutic regimen with a single injection of the APC and two light exposures to maximize therapeutic effects.

Fractionated dosing of the APC with repeated light exposure is also likely to increase effectiveness. For instance, in a model utilizing EGFR-targeted NIR-PIT repeated dosing of the APC and NIR light dosing was reported to improve the therapeutic effect compared to a single shot approach (Mitsunaga et al., 2012; Nagaya et al., 2015). Therefore, we investigated this regimen of repeated APC and NIR exposure in this aggressive lymphoma. This proved to be an effective therapy for treating a CD20 expressing tumor model despite its aggressive growth pattern. Looking forward to NIR-PIT use in humans with B-cell lymphomas, splitting the APC dose and using repeated light exposures will reduce toxicity of drugs. One significant advantage of NIR-PIT is that non-target expressing cells immediately

adjacent to targeted cells show no toxic effects because NIR light exposure by itself is harmless (Mitsunaga et al., 2011). Additionally, IR700 by itself or catabolites of APC containing IR700 does not show any phototoxicity to cells *in vitro* probably due to the hydrophilicity and excrete more than 95% into urine within 6 h after injecting into the circulation. Thus IR700 itself does not show any tumor accumulation or any anti-tumor effects *in vivo* (Mitsunaga et al., 2011; Sato et al., 2014), so that we still address IR700 as a photo-absorber rather than photosensitizer because of no photosensitizing effect. Therefore, repeated APC and NIR light administration will maximize the efficacy greater than the naked rituximab antibody therapy without increasing toxicity unlike Y-90 labeled CD20-targeted radioimmunotherapy that showed a dose-limiting bone marrow toxicity.

In this study, we saw a greater therapeutic effect in Ramos tumors compared to Daudi tumors *in vivo*. Ramos tumors had higher APC accumulation than Daudi cells although Daudi cells were more sensitive to NIR-PIT than Ramos cells at the same NIR light doses *in vitro*. This data shows the importance of APC uptake within the tumor. The IR700 fluorescence signal

reflects the concentration of APC within the tumor and therefore may be of prognostic value. These results suggest that the therapeutic effect induced by NIR-PIT depends not only on sensitivity of individual cells *in vitro* but also on the access of APCs to targeted tumor cells *in vivo*.

There are several limitations of the proposed approach. An obvious limitation is the limited penetration of NIR light within tissue. Since many lymphomas are in deep tissues, NIR-PIT may not be possible. However, some lymphomas such as mycosis fungoides, which is a T-cell lymphoma frequently expressing CD25, are located superficially and would be readily amenable to NIR-PIT. Deeper lesions are not out of the question. For instance, fiber optic light probes could be placed within tumor using endoscopes, laparoscopes, or image guided percutaneous needles. This would enable selective lymphoma masses to be effectively treated as the depth of penetration of NIR light is at least 2 cm. Thus, a fiber optic light delivery probe could potentially treat a lesion 4 cm in diameter. Moreover, multiple fiber optic probes could be inserted to treat larger lesions. Such an approach is not meant to substitute for systemic therapy but rather to address rapidly growing locoregional tumors. NIR-PIT could enable rapid inhibition of tumor growth at specific sites where a tumor is growing rapidly and uncontrollably such as near the airway or gastrointestinal tract. NIR-PIT could be used to temporize the patient until systemic therapies could be used. NIR-PIT is particularly well adapted to this task because it causes rapid and highly specific cell killing unlike many other ablative technologies. Finally, it should be noted that this study was conducted with immunocompromised mouse models. Since NIR-PIT induces a necrotic/immunogenic cell death, it can elicit host tumor immunity that may enhance the therapeutic effects (Ogawa *et al.*, 2016). However, the degree to which tumor immunity plays a role in lymphomas is still unclear. Nevertheless, to the extent it is important, NIR-PIT would be a strongly positive stimulus for additional therapeutic efficacy.

## 5. Conclusions

The conjugate rit-IR700 showed accumulation in CD20 expressing lymphoma cells. Subsequent NIR-PIT using rit-IR700 induced remarkable therapeutic responses in two animal tumor models of CD20 expressing B-cell lymphoma and cured more than half of lymphomas with this single regimen of NIR-PIT.

## Conflicts of interest

None declared.

## Acknowledgments

This research was supported by the Intramural Research Program of the National Institutes of Health, National Cancer Institute, Center for Cancer Research (ZIA BC011513).

## REFERENCES

- Economopoulos, T., Fountzilas, G., Pavlidis, N., Kalantzis, D., Papageorgiou, E., Christodoulou, C., Hamilos, G., Nicolaides, C., Dimopoulos, M., 2003. Rituximab in combination with CNOP chemotherapy in patients with previously untreated indolent non-Hodgkin's lymphoma. *Hematol. J.* 4, 110–115.
- Griffin, T.C., Weitzman, S., Weinstein, H., Chang, M., Cairo, M., Hutchison, R., Shiramizu, B., Wiley, J., Woods, D., Barnich, M., Gross, T.G., 2009. A study of rituximab and ifosfamide, carboplatin, and etoposide chemotherapy in children with recurrent/refractory B-cell (CD20+) non-Hodgkin lymphoma and mature B-cell acute lymphoblastic leukemia: a report from the Children's Oncology Group. *Pediatr. Blood Cancer* 52, 177–181.
- Hamaguchi, Y., Xiu, Y., Komura, K., Nimmerjahn, F., Tedder, T.F., 2006. Antibody isotype-specific engagement of Fcγ receptors regulates B lymphocyte depletion during CD20 immunotherapy. *J. Exp. Med.* 203, 743–753.
- Hanaoka, H., Nagaya, T., Sato, K., Nakamura, Y., Watanabe, R., Harada, T., Gao, W., Feng, M., Phung, Y., Kim, I., Paik, C.H., Choyke, P.L., Ho, M., Kobayashi, H., 2015. Glypican-3 targeted human heavy chain antibody as a drug carrier for hepatocellular carcinoma therapy. *Mol. Pharm.* 12, 2151–2157.
- Kobayashi, H., Watanabe, R., Choyke, P.L., 2013. Improving conventional enhanced permeability and retention (EPR) effects; what is the appropriate target? *Theranostics* 4, 81–89.
- Lefebvre, M.L., Krause, S.W., Salcedo, M., Nardin, A., 2006. Ex vivo-activated human macrophages kill chronic lymphocytic leukemia cells in the presence of rituximab: mechanism of antibody-dependent cellular cytotoxicity and impact of human serum. *J. Immunother.* 29, 388–397.
- Leget, G.A., Czuczman, M.S., 1998. Use of rituximab, the new FDA-approved antibody. *Curr. Opin. Oncol.* 10, 548–551.
- Marcus, R., Imrie, K., Belch, A., Cunningham, D., Flores, E., Catalano, J., Solal-Celigny, P., Offner, F., Walewski, J., Raposo, J., Jack, A., Smith, P., 2005. CVP chemotherapy plus rituximab compared with CVP as first-line treatment for advanced follicular lymphoma. *Blood* 105, 1417–1423.
- Mitsunaga, M., Nakajima, T., Sano, K., Choyke, P.L., Kobayashi, H., 2012. Near-infrared theranostic photoimmunotherapy (PIT): repeated exposure of light enhances the effect of immunoconjugate. *Bioconjug. Chem.* 23, 604–609.
- Mitsunaga, M., Ogawa, M., Kosaka, N., Rosenblum, L.T., Choyke, P.L., Kobayashi, H., 2011. Cancer cell-selective *in vivo* near infrared photoimmunotherapy targeting specific membrane molecules. *Nat. Med.* 17, 1685–1691.
- Molyneux, E.M., Rochford, R., Griffin, B., Newton, R., Jackson, G., Menon, G., Harrison, C.J., Israels, T., Bailey, S., 2012. Burkitt's lymphoma. *Lancet* 379, 1234–1244.
- Nagaya, T., Nakamura, Y., Sato, K., Harada, T., Choyke, P.L., Kobayashi, H., 2016a. Improved micro-distribution of antibody-photon absorber conjugates after initial near infrared photoimmunotherapy (NIR-PIT). *J. Control Release* 232, 1–8.
- Nagaya, T., Nakamura, Y., Sato, K., Zhang, Y.F., Ni, M., Choyke, P.L., Ho, M., Kobayashi, H., 2016b. Near infrared photoimmunotherapy with an anti-mesothelin antibody. *Oncotarget* 7, 23361–23369.
- Nagaya, T., Sato, K., Harada, T., Nakamura, Y., Choyke, P.L., Kobayashi, H., 2015. Near infrared photoimmunotherapy targeting EGFR positive triple negative breast cancer: optimizing the conjugate-light regimen. *PLoS One* 10, e0136829.
- Ogawa, M., Tomita, Y., Nakamura, Y., Lee, M.-J., Lee, S., Tomita, S., Nagaya, T., Sato, K., Yamauchi, T., Iwai, H.,

- Kumar, A., Haystead, T., Shroff, H., Choyke, P.L., Trepel, J.B., Kobayashi, H., 2016. Immunogenic Cancer Cell Death Selectively Induced by Near-infrared Photoimmunotherapy (In submission).
- Reff, M.E., Carner, K., Chambers, K.S., Chinn, P.C., Leonard, J.E., Raab, R., Newman, R.A., Hanna, N., Anderson, D.R., 1994. Depletion of B cells in vivo by a chimeric mouse human monoclonal antibody to CD20. *Blood* 83, 435–445.
- Sano, K., Nakajima, T., Choyke, P.L., Kobayashi, H., 2013. Markedly enhanced permeability and retention effects induced by photoimmunotherapy of tumors. *ACS Nano* 7, 717–724.
- Sano, K., Nakajima, T., Choyke, P.L., Kobayashi, H., 2014. The effect of photoimmunotherapy followed by liposomal daunorubicin in a mixed tumor model: a demonstration of the super-enhanced permeability and retention effect after photoimmunotherapy. *Mol. Cancer Ther.* 13, 426–432.
- Sato, K., Watanabe, R., Hanaoka, H., Harada, T., Nakajima, T., Kim, I.S., Paik, C.H., Choyke, P.L., Kobayashi, H., 2014. Photoimmunotherapy: comparative effectiveness of two monoclonal antibodies targeting the epidermal growth factor receptor. *Mol. Oncol.* 8, 620–632.
- Sato, K., Nagaya, T., Mitsunaga, M., Choyke, P.L., Kobayashi, H., 2015. Near infrared photoimmunotherapy for lung metastases. *Cancer Lett.* 365, 112–121.
- Tedder, T.F., Engel, P., 1994. CD20: a regulator of cell-cycle progression of B lymphocytes. *Immunol. Today* 15, 450–454.
- Uchida, J., Hamaguchi, Y., Oliver, J.A., Ravetch, J.V., Poe, J.C., Haas, K.M., Tedder, T.F., 2004. The innate mononuclear phagocyte network depletes B lymphocytes through Fc receptor-dependent mechanisms during anti-CD20 antibody immunotherapy. *J. Exp. Med.* 199, 1659–1669.
- Wasterlid, T., Brown, P.N., Hagberg, O., Hagberg, H., Pedersen, L.M., D'Amore, F., Jerkeman, M., 2013. Impact of chemotherapy regimen and rituximab in adult Burkitt lymphoma: a retrospective population-based study from the Nordic Lymphoma Group. *Ann. Oncol.* 24, 1879–1886.
- Wasterlid, T., Jonsson, B., Hagberg, H., Jerkeman, M., 2011. Population based study of prognostic factors and treatment in adult Burkitt lymphoma: a Swedish Lymphoma Registry study. *Leuk. Lymphoma* 52, 2090–2096.
- Watanabe, R., Hanaoka, H., Sato, K., Nagaya, T., Harada, T., Mitsunaga, M., Kim, I., Paik, C.H., Wu, A.M., Choyke, P.L., Kobayashi, H., 2015. Photoimmunotherapy targeting prostate-specific membrane antigen: are antibody fragments as effective as antibodies? *J. Nucl. Med.* 56, 140–144.
- Wildes, T.M., Farrington, L., Yeung, C., Harrington, A.M., Foyil, K.V., Liu, J., Kreisel, F., Bartlett, N.L., Fenske, T.S., 2014. Rituximab is associated with improved survival in Burkitt lymphoma: a retrospective analysis from two US academic medical centers. *Ther. Adv. Hematol.* 5, 3–12.